Progress In Electromagnetics Research Letters, Vol. 44, 29–34, 2014

Compact LPF with Sharp Roll Off and Wide Stopband using Coupling Stepped Impedance Triangular Resonator

Zebao Du*, Hao Yang, Haiying Zhang, and Min Zhu

Abstract—A lowpass filter with sharp transition and wide stopband using a novel coupling stepped-impedance triangular resonator is presented. The *L*-*C* equivalent circuit is developed for designing this type filter and analyzing the mechanism for improving roll-off and rejection property. The stopband width, passband edge, roll-off rate and overall suppression level are affected by coupling capacitance. The effect of coupling capacitance is analyzed using calculated frequency response. Coupling triangular stubs provide adequate coupling capacitance resulting in balance among transition property, stopband width and suppression level easily. A single LPF unit is designed and fabricated with cutoff frequency of 860 MHz. The single LPF unit exhibits 40-dB suppression level from 1.11 GHz to 2.28 GHz. A cascaded LPF with three asymmetric units provides 40-dB suppression level from 1.1 GHz to 6.76 GHz, and roll-off rate of 154 dB/GHz with compact size as small as $0.23\lambda_g \times 0.05\lambda_g$, where λ_g is guided wavelength at cutoff frequency.

1. INTRODUCTION

Microwave passive circuits have been widely developed during the last few years. Lowpass filters (LPFs) are one of the most important components in modern microwave communication system. Many efforts have been explored to improve its performance, such as high rejection level, wide stopband and minimum size [1–8].

Shunt resonators have been widely used to extend the stopband width owing to its advantage of introducing at least one transmission zero in stopband with compact size. Meandered-slot dumbbell resonator and windmill resonator are presented in [1, 2], respectively. Compact LPF with wide stopband can be obtained by cascading pairs of these resonators with different size. However, they suffer from poor passband flatness and gradual transition. A novel coupling stepped-impedance resonator (SIR) was introduced to obtain a miniaturized LPF with sharp roll off [3]. However, its lower suppression level and fine process requirement restrict its application. In addition, stepped-impedance resonator, open stubs and folded high impedance transmission line were combined to realize a compact LPF with sharp transition [4]. But its stopband needs to be further improved. Cascading LPF units with different size is an effective method to extend stopband with a little size increase. Interdigital structure was embedded in low impedance section of stepped-impedance hairpin unit to control the transmission zeros location and improve stopband and transition property [5]. Two hairpin units with different size were cascaded to achieve wide stopband. But this method cannot improve its suppression level. Stopband, roll-off rate and rejection level can be improved by increasing filters' orders in LPF design. A LPF with wide stopband and high suppression level was obtained by using multiple cascaded stepped-impedance hairpin resonators [6]. But it enlarges component size and in-band loss. In this letter, appropriate filter order (five orders in this letter) and cascading technique are combined to achieve high suppression level, wide stopband and small size.

Received 22 October 2013, Accepted 18 November 2013, Scheduled 21 November 2013

* Corresponding author: Zebao Du (duzebao@ime.ac.cn).

The authors are with the Department of RFIC, Institute of Microelectronics, Chinese Academy of Sciences, No. 3, Bei-Tu-Cheng West Road, Beijing 10029, China.

In this letter, a compact LPF unit with sharp roll off, broad stopband and high rejection level is achieved with a novel application of coupling stepped-impedance triangular resonator. Meandered high impedance transmission line (HITL) is introduced to further reduce circuit size. In order to further extend the stopband width, a LPF with three cascaded asymmetric units is designed and fabricated. The equivalent circuit model is developed for designing this type of filter and explaining the mechanism for improving out-of-band rejection and roll-off rate.

2. FILTER STRUCTURE AND ANALYSIS

The proposed compact LPF is shown in Fig. 1(a). The LPF consists of SIRs and HITL. The low impedance section of SIR is implemented with triangular stub, which increases coupling strength between coupling stubs. The L-C equivalent model of the filter is shown in Fig. 1(b), where the network in Fig. 1(a) is assumed lossless. C_{p1} and C_{p2} represent the grounding capacitance of the low impedance section of SIRs. C_g denotes the coupling capacitance between triangular stubs. L_{s1} models the inductance of HITH between feed point and center loaded SIR. L_{p1} and L_{p2} represent the inductance of high impedance section of SIR1 and SIR2, respectively. C_{d1} and C_{d2} denote the parasitic capacitance due to the junction discontinuities.

The scattering parameter can be derived using even-odd mode analysis due to symmetry of equivalent circuit [9]. The circuit in Fig. 1(b) can be decomposed to superposition of an even-mode and odd-mode excitations, as shown in Fig. 2. C_{d1} and C_{d2} are very small that they mainly affect the frequency response at upper frequency. In order to simplify the analysis of transmission zeros and cutoff property, they have been neglected in even-odd mode analysis.

It is assumed that a wave of unit amplitude is incident at port 1. The amplitudes of emerging wave at each port of the L-C circuit can be expressed:

$$E_1 = 1/2(\Gamma_e + \Gamma_o) \quad (1)$$

$$E_2 = 1/2(\Gamma_e - \Gamma_o) \quad (2)$$

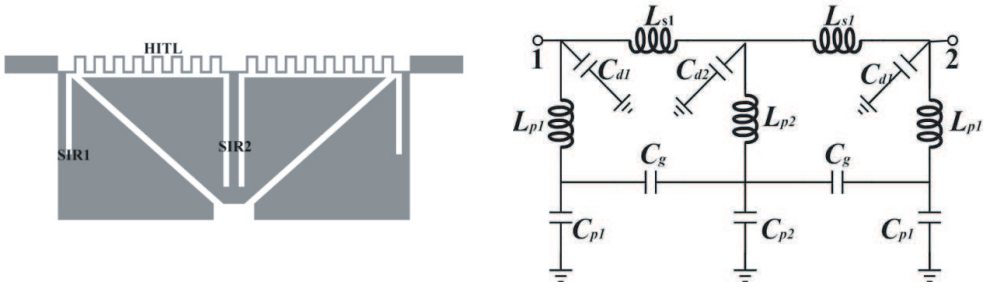

Figure 1. (a) LPF structure and (b) its L-C equivalent circuit.

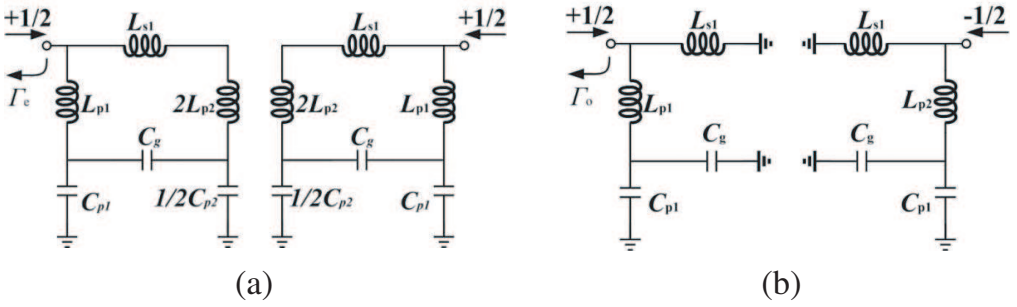

Figure 2. (a) Even-mode excitation. (b) Odd-mode excitation.

E_1 and E_2 are the amplitudes of emerging wave at port 1 and port 2, respectively. Γ_e and Γ_o are even- and odd-mode reflection coefficients for the even-odd mode circuits in Fig. 2. Then the scattering parameter of the LPF can be derived as:

$$S_{21} = E_2 = \frac{(Z_e - Z_o)Z_s}{(Z_e + Z_s)(Z_o + Z_s)} \tag{3}$$

$$S_{11} = E_1 = \frac{Z_o Z_e - Z_s^2}{(Z_e + Z_s)(Z_o + Z_s)} \tag{4}$$

Z_s, Z_e and Z_o are source impedance, even- and odd-mode input impedances, respectively. The even- and odd-mode input impedances can be expressed as:

$$Z_o = \frac{j\omega\left[L_{s1} - \omega^2 L_{p1} L_{s1}(C_g + C_{p1})\right]}{1 - \omega^2(L_{p1} + L_{s1})(C_g + C_{p1})} \tag{5}$$

$$Z_e = \frac{Z_1 Z_2 + Z_1 Z_3 + Z_2 Z_3 - 2/(\omega^2 C_{p1} C_{p2})}{Z_1 + Z_2 - j/(\omega C_{p1}) - j2/(\omega C_{p2})} - \frac{j(Z_2 + Z_3)/(\omega C_{p1}) + j2(Z_1 + Z_3)/(\omega C_{p2})}{Z_1 + Z_2 - j/(\omega C_{p1}) - j2/(\omega C_{p2})} \tag{6}$$

$$Z_1 = L_{p1}/(C_g Z_{de}) \tag{7}$$

$$Z_2 = (L_{s1} + 2L_{p2})/(C_g Z_{de}) \tag{8}$$

$$Z_3 = -\omega^2(L_{s1} + 2L_{p2})L_{p1}/Z_{de} \tag{9}$$

$$Z_{de} = j\omega(L_{s1} + 2L_{p2} + L_{p1}) - j/(\omega C_g) \tag{10}$$

In Eq. (3), the intersection of Z_e and Z_o means transmission zeros in stopband. In order to achieve high suppression level, the even- and odd-mode input impedances have to be close to each other in the stopband. As shown in Fig. 3, the even- and odd-mode input impedances are calculated from (5) to (10) with different coupling capacitance. Once coupling capacitance is introduced, approximately equal range of Z_e and Z_o extend to cutoff frequency which improves transition property.

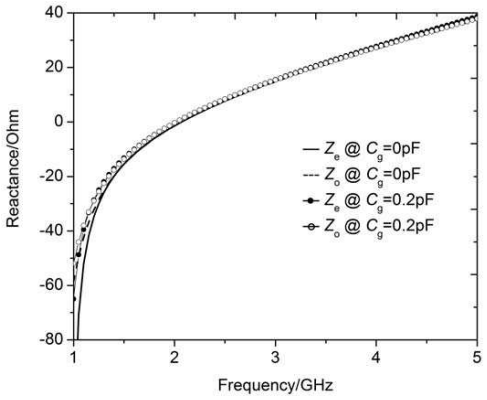

Figure 3. Even- and odd-mode input impedances ($L_{s1} = 12\,\text{nH}$, $L_{p1} = 1.6\,\text{nH}$, $L_{p2} = 2\,\text{nH}$, $C_{p1} = 3.7\,\text{pF}$ and $C_{p2} = 5.8\,\text{pF}$).

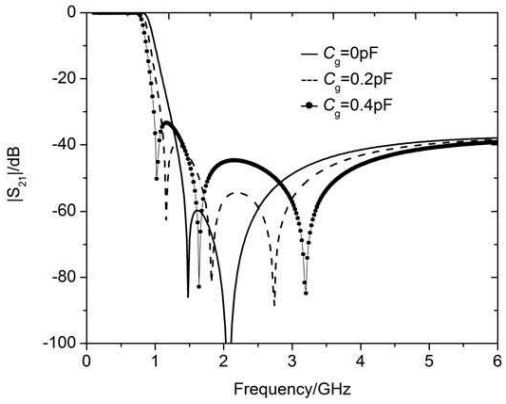

Figure 4. Calculated frequency response with different C_g ($L_{s1} = 12\,\text{nH}$, $L_{p1} = 1.6\,\text{nH}$, $L_{p2} = 2\,\text{nH}$, $C_{p1} = 3.7\,\text{pF}$ and $C_{p2} = 5.8\,\text{pF}$).

The calculated frequency response based on different coupling capacitance C_g is shown in Fig. 4. As depicted from the solid line, only two transmission zeros are produced from the SIRs. Once coupling capacitance is introduced between SIRs, one more transmission zero is introduced to be closed to passband. The first and second transmission zero shift to lower frequency along with bigger coupling capacitance. The third transmission zero shifts to higher frequency at the same time. But a larger coupling capacitance results in higher fluctuation between the first and second transmission zeros, which worsen the overall suppression level. An adequate coupling capacitance provides a balance among high suppression level, broad stopband and sharp transition. In this design, the coupling triangular stubs are introduced to achieve optimal coupling capacitance. Compared with conventional coupling rectangular

stubs, the coupling triangular stubs provide bigger coupling capacitance resulting in sharper transition. In addition, the coupling triangular stubs provide smaller coupling capacitance and simple structure compared with interdigital structure, which results in higher overall suppression level.

3. DESIGN AND RESULTS

A five-order Chebyshev *L*-*C* LPF prototype with 0.02-dB ripple and 860-MHz cutoff frequency is developed at first. Secondly the shunt capacitors are transformed to series resonant circuits based on transmission zeros location and their reactance in the passband. Then the *L*-*C* values are tuned and optimized using Advanced Design System (ADS). In this design, the initial values of the LPF are obtained as follows: $L_{s1} = 12\,\text{nH}$, $L_{p1} = 1.6\,\text{nH}$, $L_{p2} = 2\,\text{nH}$, $C_{p1} = 3.7\,\text{pF}$, $C_{p2} = 5.8\,\text{pF}$. As depicted from Fig. 4, a smaller coupling capacitance can improve transition and stopband property without changing passband.

The inductors in *L*-*C* circuit can be transformed to HITL, and the grounding capacitors can be transformed to open stubs simultaneously [10]. The physical dimensions of microstrip lines have to be optimized using electromagnetic (EM) simulation because of the parasitic and coupling effect. The LPF is designed and fabricated on the Rogers 4003 substrate with thickness of 0.508 mm and relative dielectric constant of 3.55. The Agilent Momentum is used for EM simulation, dimension tuning and optimization. The photograph of the proposed LPF is shown in Fig. 5(a). The component size of the LPF is $20.8\,\text{mm} \times 10.15\,\text{mm}$, i.e., $0.1\lambda_g \times 0.05\lambda_g$ where λ_g is guided wavelength at cutoff frequency. The fabricated LPF is measured with HP8720ES vector network analyzer. The simulated and measured results are illustrated in Fig. 5(b). The measured results show that the proposed LPF have a sharp transition and high suppression level. The measured rejection is better than 40 dB from 1.11 GHz to 2.28 GHz, except the fluctuation of 37.7 dB recorded at 1.28 GHz. The roll-off rate is as higher as 148 dB/GHz.

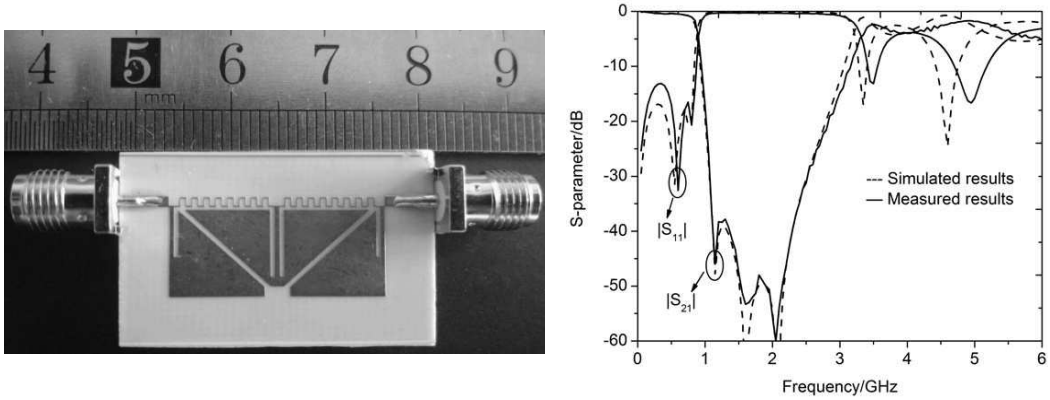

Figure 5. (a) photograph of single LPF unit. (b) Simulated and measured results of single LPF unit.

In order to further extend the stopband width, a LPF with three cascaded asymmetrical units is designed. The first unit is the same with the above single one, which mainly controls the cutoff frequency property. The second unit is introduced to extend the stopband. The third one is proposed to further increase rejection level. Its layout with dimensions in millimeter is shown in Fig. 6(a). The photograph of the proposed LPF is shown in Fig. 6(b). Fig. 6(c) shows the simulated and measured results of the fabricated cascaded LPF. The new LPF demonstrates good measured characteristics including a wide stopband from 1.1 GHz to 6.76 GHz with a very high suppression level more than 40 dB. The roll-off rate is 154 dB/GHz (attenuation: 3 dB at 0.86 GHz and 40 dB at 1.1 GHz). The size of cascaded LPF is $0.23\lambda_g \times 0.05\lambda_g$. The measured results are summarized with previously reported high performance LPFs, as shown in Table 1. The proposed cascaded LPF exhibits high suppression level, sharp roll-off rate, wide stopband and small size.

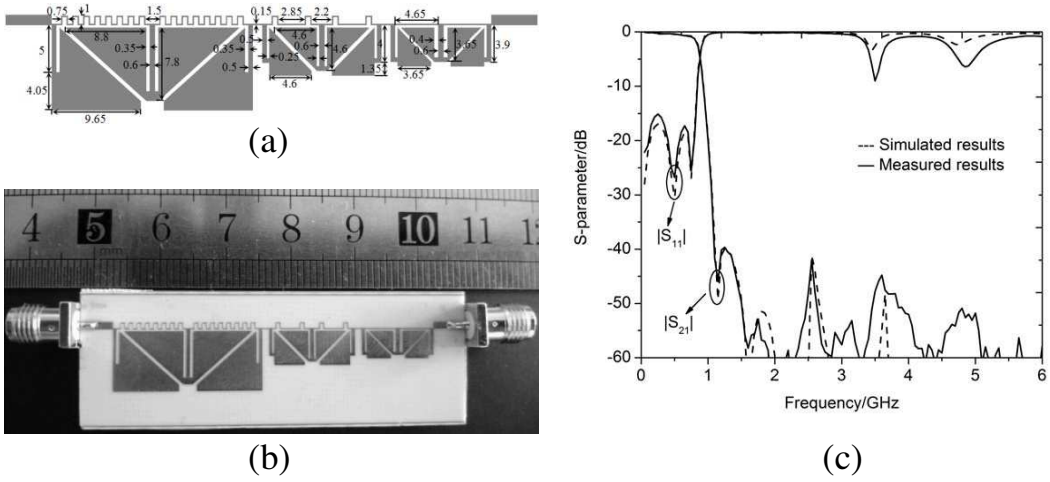

Figure 6. (a) Layout of cascaded LPF. (b) Photograph of cascaded LPF. (c) Simulated and measured results of cascaded LPF.

Table 1. Comparison with previously reported high performance LPFs.

Ref.	f_c (GHz)	SL (dB)	ST, times	ROR (dB/GHz)	Size (λ_g^2)
[2]	1.76	20	12.3,7	51.5	0.048
[4]	2.49	20	7, 2.8	49	0.032
[5]	1.0	20	5.5, 5.5	74	0.012
[6]	2.0	33.3	10, 5	67.3	Large
[7]	0.53	20	4.6, 8.7	95	0.022
[8]	3	25	24, 8	48	0.062
This work	**0.86**	**40**	**6.76, 7.8**	**154**	**0.012**

f_c: cutoff frequency; SL: suppression level; ST: stopband up to (GHz); Times = ST/f_c; ROR: roll-off rate.

4. CONCLUSION

A novel compact LPF structure with coupling triangular stubs has been proposed in this letter. Coupling triangular stubs provide not only adequate coupling capacitance, but also very compact size simultaneously. The meandered line is introduced to further reduce the component size. A single-unit LPF and a cascaded LPF have been designed, fabricated and measured. The measured results of cascaded LPF show some advantages such as sharp roll-off rate, wide stopband, high suppression level and small size.

REFERENCES

1. Cao, H. L., W. B. Ying, H. Li, and S. Z. Yang, "Compact lowpass filter with ultra-wide stopband rejection using meandered-slot dumbbell resonator," *Journal of Electromagnetic Waves and Applications*, Vol. 26, Nos. 17–18, 2203–2210, Dec. 2012.
2. Cao, H., W. Ying, H. Li, and S. Yang, "Compact lowpass filter with wide stopband using novel windmill resonator," *Journal of Electromagnetic Waves and Applications*, Vol. 26, Nos. 17–18, 2234–2241, Dec. 2012.

3. Hayati, M., S. Roshani, S. Roshani, and F. Shama, "A novel miniaturized Wilkinson power divider with nth harmonic suppression," *Journal of Electromagnetic Waves and Applications*, Vol. 27, No. 6, 726–735, Apr. 2013.
4. Yang, R. Y., Y. L. Lin, C. Y. Hung, and C. C. Lin, "Design of a compact and sharp-rejection low-pass filter with a wide stopband," *Journal of Electromagnetic Waves and Applications*, Vol. 26, Nos. 17–18, 2284–2290, Dec. 2012.
5. Li, L., Z. F. Li, and J. F. Mao, "Compact lowpass filters with sharp and expanded stopband using stepped impedance hairpin units," *IEEE Microw. Wireless Compon. Lett.*, Vol. 20, No. 6, 310–312, Jun. 2010.
6. Hsieh, L. H. and K. Chang, "Compact elliptic-function low-pass filters using microstrip stepped-impedance hairpin resonators," *IEEE Trans. on Microw. Theory and Tech.*, Vol. 51, No. 1, 193–199, Jan. 2003.
7. Velidi, V. K. and S. S. Sanyal, "Sharp roll-off lowpass filters with wide stopband using stub-loaded coupled-line hairpin unit," *IEEE Microw. Wireless Compon. Lett.*, Vol. 21, No. 6, 301–303, Jun. 2011.
8. Ma, K. and K. S. Yeo, "New ultra-wide stopband low-pass filter using transformed radial stubs," *IEEE Trans. on Microw. Theory and Tech.*, Vol. 59, No. 3, 604–611, Mar. 2011.
9. David, M. P., *Microwave Engineering*, 3rd Edition, New York, 2005.
10. Hong, J. S. and M. J. Lancaster, *Microstrip Filters for RF/Microwave Applications*, Wiley, New York, 2001.